Brazilian Journal of Medical and Biological Research (2006) 39: 1549-1562
ISSN 0100-879X

Proteomic inventory of myocardial proteins from patients with chronic Chagas' cardiomyopathy

P.C. Teixeira[1,3,4], L.K. Iwai[1,4], A.C.K. Kuramoto[1,4], R. Honorato[2], A. Fiorelli[2], N. Stolf[2], J. Kalil[1,3,4] and E. Cunha-Neto[1,3,4]

[1]Laboratório de Imunologia, [2]Divisão de Cirurgia Torácica, Instituto do Coração, Hospital das Clínicas, [3]Disciplina de Imunologia Clínica e Alergia, Faculdade de Medicina, Universidade de São Paulo, São Paulo, SP, Brasil
[4]Instituto de Investigação em Imunologia, Instituto do Milênio, CNPq/MCT, São Paulo, SP, Brasil

Abstract

Chronic Chagas' disease cardiomyopathy (CCC) is an often fatal outcome of *Trypanosoma cruzi* infection, with a poorer prognosis than other cardiomyopathies. CCC is refractory to heart failure treatments, and is the major indication of heart transplantation in Latin America. A diffuse myocarditis, plus intense myocardial hypertrophy, damage and fibrosis, in the presence of very few *T. cruzi* forms, are the histopathological hallmarks of CCC. To gain a better understanding of the pathophysiology of CCC, we analyzed the protein profile in the affected CCC myocardium. Homogenates from left ventricular myocardial samples of end-stage CCC hearts explanted during heart transplantation were subjected to two-dimensional electrophoresis with Coomassie blue staining; protein identification was performed by MALDI-ToF mass spectrometry and peptide mass fingerprinting. The identification of selected proteins was confirmed by immunoblotting. We demonstrated that 246 proteins matched in gels from two CCC patients. They corresponded to 112 distinct proteins. Along with structural/contractile and metabolism proteins, we also identified proteins involved in apoptosis (caspase 8, caspase 2), immune system (T cell receptor ß chain, granzyme A, HLA class I) and stress processes (heat shock proteins, superoxide dismutases, and other oxidative stress proteins). Proteins involved in cell signaling and transcriptional factors were also identified. The identification of caspases and oxidative stress proteins suggests the occurrence of active apoptosis and significant oxidative stress in CCC myocardium. These results generated an inventory of myocardial proteins in CCC that should contribute to the generation of hypothesis-driven experiments designed on the basis of the classes of proteins identified here.

Correspondence
E. Cunha-Neto
Laboratório de Imunologia
InCor-HC-FM, USP
Av. Dr. Eneas C. Aguiar, 44
Bloco II, 9º andar
05403-000 São Paulo, SP
Brasil
Fax: +55-11-3069-5953
E-mail: edecunha@gmail.com

Research supported by FAPESP (Nos. 00/14549-4 and 01/00729-3). P.C. Teixeira is supported by a FAPESP grant (No. 04/15322-4), and E. Cunha-Neto and J. Kalil are recipients of productivity awards from CNPq (Nos. 302970-2004-5 and 307541-2003-7).

Received December 20, 2005
Accepted August 23, 2006

Key words
- Chagas' disease
- Cardiomyopathy
- Proteomic analysis
- Two-dimensional electrophoresis
- MALDI-ToF

Introduction

Chagas' disease is a significant cause of morbidity and mortality in Central and South America, affecting about 13 million people (1). The disease is caused by infection with the intracellular protozoan parasite *Trypanosoma cruzi*. About 30% of Chagas' disease patients develop chronic Chagas' disease cardiomyopathy (CCC), an inflammatory cardiomyopathy that occurs decades after the initial infection, and one-third progress further to a particularly aggressive, life-threatening dilated cardiomyopathy. In spite of the recent advances in vector control, the millions of patients already infected deserve more attention from the scientific community. Furthermore, clinical progression, length of survival and overall prognosis are significantly worse in CCC patients compared with patients with dilated cardiomyopathy of non-inflammatory etiology (2,3).

CCC heart lesions show histopathological findings consistent with inflammation and a myocardial remodeling process: T cell/macrophage-rich myocarditis, hypertrophy, and fibrosis with heart fiber damage (4). The local cytokine production profile is consistent with a T1-type response, with interferon-gamma (γ)-induced chemokines (5-12). Gene expression profiling of CCC myocardial tissues showed that 15% of the known genes selectively up-regulated in CCC are IFN-γ-inducible (12). Exposure of cardiomyocytes to IFN-γ can up-regulate the expression of atrial natriuretic factor (12), suggesting that IFN-γ may directly modulate gene expression in myocardial cells. These results are consistent with a possible role of IFN-γ-induced chronic inflammation in modulating myocardial gene expression.

However, gene expression profiling may not be faithfully reflected at the protein level. Advances in two-dimensional (2-D) electrophoresis, mass spectrometry, and bioinformatics, along with progress in genomic sequence analysis now make possible a direct evaluation of large-scale protein profiles (13).

In order to study the global protein profile of the myocardium under the effect of chronic inflammation in CCC heart tissue, and to gain insight about the pathophysiology of CCC, we analyzed the myocardial proteome from end-stage CCC patients.

Patients, Material and Methods

Reagents

Immobilized pH gradient gel buffer, trypsin (sequencing grade), α-cyano-4-hydroxycinnamic acid and other analytical grade reagents were purchased from Amersham Biosciences (Uppsala, Sweden), with the exception of ammonium bicarbonate, analytical grade acetonitrile and trifluoroacetic acid (TFA) that were obtained from Merck (Darmstadt, Germany). ACTH peptide 18-39 and (Ile7)-angiotensin III were obtained from Sigma (St. Louis, MO, USA). All stock solutions were prepared with deionized water using a Milli-Q Academic System (Millipore Co., Billerica, MA, USA).

Sample preparation

The protocol was approved by the Institutional Review Board of the University of São Paulo School of Medicine and written informed consent was obtained from the patients.

Myocardial left ventricular free wall heart samples were obtained from two end-stage heart failure CCC patients with a diagnosis established by seropositivity to *T. cruzi* in at least two of three tests, i.e., ELISA, indirect immunofluorescence and indirect hemagglutination, and by positive epidemiology. Both patients were female and were 42 and 62 years old, with an ejection fraction <40%. The hearts were explanted on the occasion of heart transplantation at the Heart Institute - InCor, University of São Paulo School of Medicine, São Paulo, SP, Brazil. Samples

were dissected, frozen in liquid nitrogen and stored at -80ºC. The tissue (100 mg) was homogenized in 1% SDS (w/v) and 0.5 mM TLCK (1 mL), submitted to three sonication cycles and centrifuged at 12,000 *g* for 15 min at 4ºC (14). The samples were passed through Millipore Centricon YM-3 filters (molecular mass cutoff at 3000 Da) and the protein content of the supernatant solution of each extract was quantified by the bicinchoninic acid method (15).

Two-dimensional gel electrophoresis

Isoelectric focusing was carried out on 24-cm long immobilized pH gradient gel strips, with a pH range of 3.0 to 10.0 (Immobiline DryStrip gels, Amersham Biosciences). The strips were rehydrated in 8 M urea, 0.5% CHAPS, 0.5% IPG buffer, 0.2% DTT, and traces of bromophenol blue containing 1 mg of cardiac protein extract for 12 h at 20ºC. Isoelectric focusing was performed using the Ettan IPGphor Isoelectric Focusing System (Amersham Biosciences) at 20ºC at 50 mA/strip in an increasing voltage gradient (500 V for 1 h, 1000 V for 1 h, and 8000 V for 8 h, accumulating a total of 64,000 Vh), according to manufacturer instructions. Before the second dimension electrophoresis, the strips were equilibrated twice for 15 min in a buffer containing 50 mM Tris, pH 8.8, 6 M urea, 30% glycerol (v/v), 2% SDS (w/v), 0.002% bromophenol blue (w/v), and in the presence of 10 mg/mL DTT in the first step and 25 mg/mL iodoacetamide in the second step. The second dimension was carried out on a vertical DaltSix system (Amersham Biosciences) at 20ºC on 12.5% polyacrylamide gels (24 x 18 cm) for 5 h at 100 W. Coomassie blue-stained gels were digitized with an ImageScanner and analyzed with the ImageMaster 2D Elite 3.10 software (Amersham Biosciences). The matching spots in the two samples were selected and the volume (related to the quantity of protein) of each spot was normalized on the basis of total volume of all spots in each gel.

Protein digestion

All spots visualized in each gel were excised, subjected to tryptic digestion and processed in a robotic workstation (Ettan Spot Handling Workstation, Amersham Biosciences). Briefly, spots (1.4 mm in diameter) were excised from the gel and then washed in 50 mM ammonium bicarbonate (NH_4HCO_3) in 50% acetonitrile (ACN) until complete destaining and SDS removal and then dried. Dehydrated gel plugs were rehydrated with 30 µL of a solution containing 0.3 µg trypsin in 20 mM NH_4HCO_3. Digestion was performed at 37ºC for 6 h. Digested peptides were extracted by the addition of 50 µL 50% ACN/0.5% TFA at room temperature for 1 h. The procedure was repeated and the supernatants were combined. Samples were concentrated and resuspended in 5 µL 5% ACN/2.5% TFA.

Protein identification

Tryptic fragments were analyzed with the Ettan MALDI-ToF Pro mass spectrometer (Amersham Biosciences). For peptide mass fingerprinting (PMF) analysis, a small quantity of each processed sample (0.5 µL) corresponding to a spot was applied on a metal slide mixed with the same quantity of matrix (α-cyano-4-hydroxycinnamic acid) and taken to the mass spectrometer for analysis. To ensure maximal accuracy, trypsin autolysis peptides (842.51 and 2211.10 Da) were used for internal mass calibration and (Ile7)-angiotensin III (897.53 Da) and ACTH peptide 18-39 (2465.20 Da) were used for external calibration of the instrument. The m/z values for trypsin autolysis peptides and for contaminants (842.5, 1045.8, 1066.4, 2211.1, 2225.1, and 2299.2) were excluded from the list of tryptic peptides representing the PMF of proteins.

Proteins were identified by comparing the PMF of each spot to virtual tryptic digestion of proteins using the MALDI-ToF Evaluation software (Amersham Biosciences) and the non-redundant NCBI databank (*H. sapiens*), using as search parameters 0.2-Da peptide mass tolerance and 1 maximum missed cleavage sites. The mass lists of each spectrum were also submitted to the Mascot tool (http://www.matrixscience.com) and Swiss-Prot databank (*H. sapiens*) with mass tolerance of 0.5 Da and 1 maximum missed cleavage as parameters. The only allowed post-translational modification was oxidation. We considered expectation values ≤0.1 as significant protein identifications. After protein identification in both gels, a composite image of the two gels was constructed by matching the spots. We could enumerate the protein spots that were matched and identified as the same protein in the two gels, as well as those that were only identified in one of the gels. The functional classification of the proteins identified in both gels was adapted from the Gene Ontology classification using the FatiGO tool (http://fatigo. bioinfo.cipf.es).

Western blot analysis

Cardiac tissue homogenates in SDS-PAGE sample buffer were heated (95ºC, 5 min), run on SDS-polyacrylamide gels and then blotted onto nitrocellulose membranes. Next, the membranes were incubated with monoclonal antibodies against heat shock protein 60, protein disulfide isomerase, Cu/Zn superoxide dismutase, caspase 8 (Stressgen Bioreagents, Victoria, British Columbia, Canada) and caspase 2 (rabbit polyclonal antibody). Antibodies were kindly provided by Drs. Celio X. Santos, Francisco Laurindo, and Gustavo Amarante-Mendes (University of São Paulo). After incubation with the appropriate horseradish peroxidase-coupled conjugate, blots were developed by chemiluminescence using ECL Plus Western Blotting Detection Reagents (Amersham Biosciences, Little Chalfont, Buckinghamshire, UK).

Results

Two-dimensional electrophoresis of the myocardium from CCC patients allowed us to observe ca. 400 spots on each gel (Figure 1). Using MALDI-ToF analysis with SWISS-PROT and the non-redundant NCBI databases, we identified proteins in 316 spots on the gel from patient 1 and 259 spots on the gel from patient 2, 246 of which were matched on both gels. Of the identified proteins, 112 were distinct proteins (Table 1). A representative spectrum of the tryptic fragments of a protein is shown in Figure 2, illustrating the mass/charge values from the trypsin autolysis products.

Table 2 shows the distribution of the 112 distinct proteins among functional categories according to the Gene Ontology classification (http://fatigo. bioinfo.cipf.es). As expected, proteins of the contractile apparatus and involved in energy generation were among the most abundant groups in CCC heart tissue. This analysis was able to identify less abundantly expressed proteins, such as transcriptional factors and proteins produced by the inflammatory infiltrate and related to the apoptotic process.

Structural proteins (19% of all distinct proteins) included multiple constituents of the sarcomeric actomyosin complex (15 proteins) such as heavy and light chains of cardiac myosin, several isoforms of actin, troponin and tropomyosin, actin-binding and Z-band proteins, as well as cytoskeletal proteins (6 proteins). The atrial isoform of myosin light chain (MYL4), which is normally suppressed after birth (16), was identified in the ventricular CCC samples. We identified six spots corresponding to vimentin, which is expressed by fibroblasts, suggesting the occurrence of a fibrotic process, a hallmark of CCC myocardium (17).

More than 38% of all distinct proteins

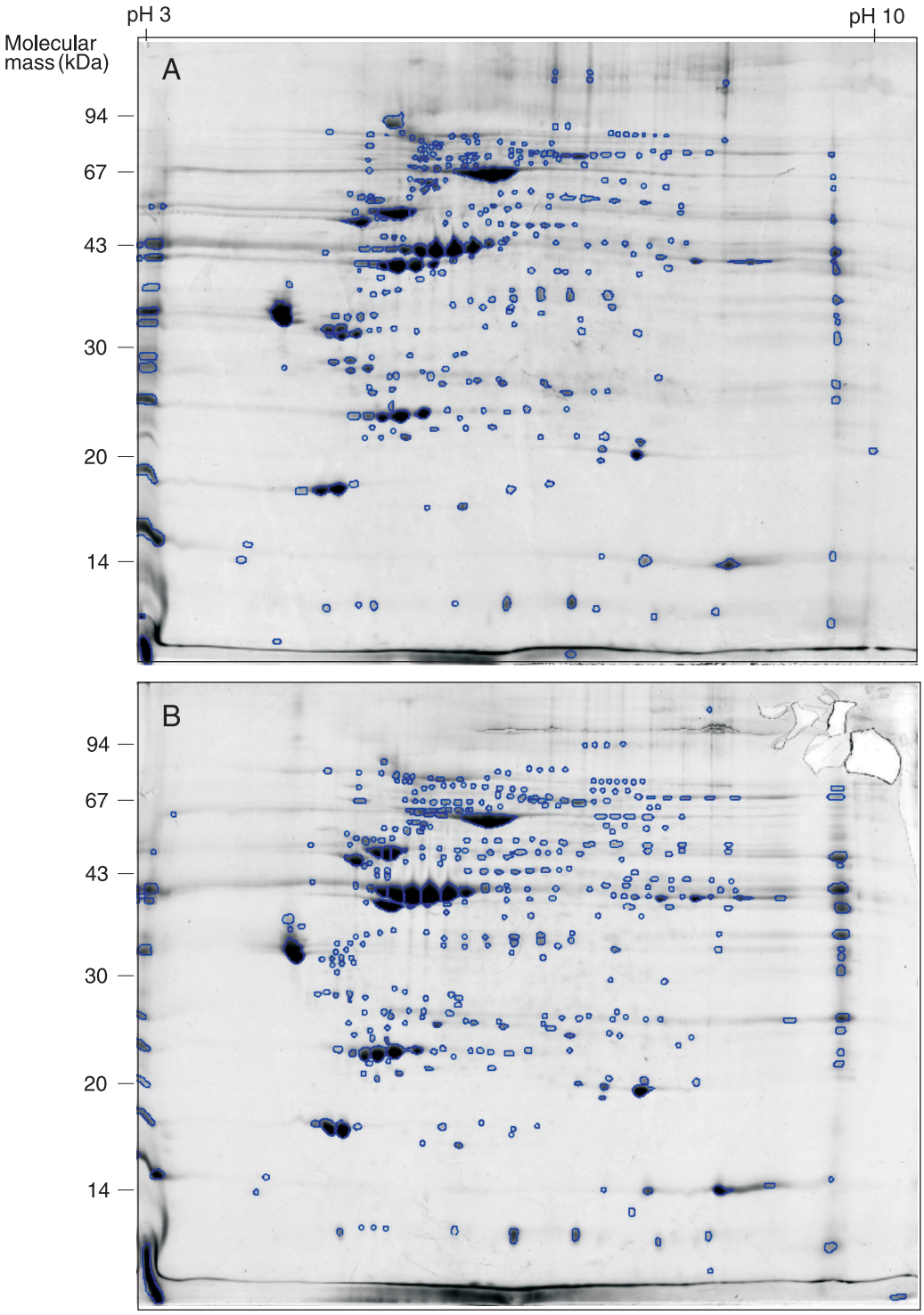

Figure 1. Two-dimensional gel electrophoresis of proteins in the myocardium of patients with chronic Chagas' disease cardiopathy (CCC). *A* and *B*, Samples from CCC patients #1 and #2; the outlines of spots that were selected for protein identification are shown. Myocardium proteins were separated by isoelectric focusing on 24-cm long immobilized pH gradient gel strips containing a linear 3-10 pH gradient, followed by SDS-PAGE on vertical 12.5% gels. Proteins were detected by Coomassie blue R-250 staining.

Table 1. Proteins identified in the myocardium of patients with chronic Chagas' disease cardiopathy by 2-D gel electrophoresis-peptide mass fingerprinting analysis.

Symbol	Description	Exp.[1]	Cov.[2] (%)	pI (T)	pI (E)	Mass (T)	Mass (E)	N. Vol.[3]	Accession number	No. Spots[4]	T. Vol.[5]
1. Structural and Contractile Proteins											
ACTA1	actin, α1, skeletal muscle	0.027	30.2	5.2	5.5	42.3	51.6	0.196	P68133	3	0.20
ACTA2	actin, α2, smooth muscle, aorta	0.010	19.7	5.3	4.8	42.3	42.1	0.034	P62736	15	0.03
ACTC	actin, α, cardiac muscle	0.006	28.1	5.2	3.0	42.3	56.0	0.816	P68032	14	0.82
ACTG2	actin, γ2, smooth muscle, enteric	0.018	34.3	5.3	5.8	42.3	54.7	3.618	P63267	8	3.62
ACTN2	actinin, α2	0.018	20.9	5.3	5.7	104.4	91.3	0.165	P35609	8	0.17
DES	desmin	0.000	41.7	5.2	5.2	53.6	65.3	1.506	P17661	13	1.51
KIAA0992	palladin	0.083	12.4	9.3	9.0	45.6	31.0	0.118	Q7Z3W0	1	0.12
LMNA	lamin A/C (70-kDa lamin)	0.010	15.0	6.3	8.4	65.0	66.2	0.037	P02545	2	0.06
MYBPC3	myosin-binding protein C, cardiac	0.001	8.8	6.2	7.5	141.8	107.2	0.030	Q14896	4	0.12
MYH6	myosin, heavy polypeptide 6, cardiac muscle, α	0.001	6.0	5.9	8.3	223.5	125.0	0.041	P13533	1	0.04
MYH7	myosin, heavy polypeptide 7, cardiac muscle, ß	0.000	33.6	5.3	5.6	183.1	75.0	0.115	P12883	12	0.79
MYL2	myosin, light polypeptide 2, regulatory, cardiac, slow	0.000	69.3	4.9	4.8	18.8	18.9	2.749	P10916	3	4.78
MYL3	myosin, light polypeptide 3, alkali, ventricular, skeletal, slow	0.000	56.2	5.0	5.3	22.0	26.9	2.636	P08590	10	7.54
MYL4	myosin, light polypeptide 4, alkali, atrial, embryonic	0.010	36.0	5.0	5.3	21.4	30.0	0.021	P12829	2	0.06
MYOZ2	myozenin 2	0.014	19.7	7.9	6.4	29.9	42.1	0.016	Q9NPC6	2	0.04
RTN2	reticulon 2	0.164	16.4	5.3	9.5	33.4	41.3	0.156	O75298	1	0.16
SSH3	slingshot homolog 3	0.059	22.0	9.5	5.3	16.5	25.8	0.017	Q8TE77	1	0.02
TNNT2	troponin T2, cardiac	0.010	20.1	4.9	5.3	33.0	51.8	4.163	P45379	3	4.49
TPM1	tropomyosin 1 (α)	0.014	34.9	4.6	4.4	26.6	42.0	5.375	P09493	2	5.59
TUBB	tubulin, ß polypeptide	0.019	19.9	4.8	5.2	30.6	69.5	0.066	P07437	1	0.07
VIM	vimentin	0.004	32.2	5.1	5.0	53.7	62.1	0.066	P08670	6	0.46
2. Metabolism											
2.1. Glycolysis											
ALDOA	fructose 1,6-biphosphate aldolase	0.020	30.0	8.8	9.5	39.7	51.3	0.821	P04075	1	0.82
ENO1	enolase 1	0.026	24.4	7.0	7.6	47.5	60.2	0.023	P06733	1	0.02
GAPDH	glyceraldehyde-3-phosphate dehydrogenase	0.019	15.2	8.7	9.5	36.2	45.6	0.665	P04406	1	0.66
LDHB	lactate dehydrogenase B	0.013	15.9	5.7	6.7	36.8	45.5	0.103	P07195	3	0.31
PDHB	pyruvate dehydrogenase, E1 beta	0.000	26.0	5.4	6.0	36.8	43.2	0.038	P11177	2	0.07
2.2. Tricarboxylic Acid Cycle											
ACO2	aconitase 2, mitochondrial	0.006	10.0	7.4	7.7	86.2	84.3	0.046	Q99798	7	0.62
DLD	dihydrolipoamide dehydrogenase precursor	0.025	22.0	7.8	8.0	54.7	66.3	0.051	P09622	3	0.18
DLST	dihydrolipoamide succinyltransferase	0.068	11.0	9.4	6.1	49.0	64.4	0.059	P36957	2	0.12
FH	fumarate hydratase precursor	0.018	23.5	9.0	8.1	54.8	58.3	0.058	P07954	4	0.17
MDH2	malate dehydrogenase 2, mitochondria	0.099	23.7	9.0	9.5	33.7	42.7	0.103	P40926	1	0.10
OGDH	oxoglutarate dehydrogenase (lipoamide)	0.015	9.3	6.6	7.3	114.7	90.4	0.027	Q02218	6	0.15
SDHA	succinate dehydrogenase complex, subunit A, flavoprotein (Fp)	0.005	14.5	7.1	7.5	73.7	77.4	0.080	P31040	4	0.30
2.3. Oxidative Phosphorylation and Electron Transport											
ATP5A1	ATP synthase, F1 complex, α polypeptide 1	0.010	21.7	9.3	9.5	59.8	64.6	0.821	P25705	2	0.82
ATP5B	ATP synthase, F1 complex, ß polypeptide	0.000	46.1	5.3	5.0	56.5	63.6	1.548	P06576	2	1.55
ATP5C1	ATP synthase, F1 complex, γ polypeptide 1	0.047	26.1	9.1	9.5	32.3	38.8	0.313	P36542	1	0.31
ETFDH	electron-transferring-flavoprotein dehydrogenase	0.002	10.1	6.9	7.9	65.5	73.6	0.013	Q16134	3	0.07

Continued on next page

Table 1 continued.

Symbol	Description	Exp.[1]	Cov.[2] (%)	pI (T)	pI (E)	Mass (T)	Mass (E)	N. Vol.[3]	Accession number	No. Spots[4]	T. Vol.[5]
NDUFS1	NADH dehydrogenase (ubiquinone) Fe-S protein 1	0.016	16.5	5.9	5.8	80.5	82.5	0.114	P28331	6	0.42
NDUFS3	NADH dehydrogenase (ubiquinone) Fe-S protein 3	0.012	27.7	7.0	6.0	30.3	30.9	0.035	O75489	2	0.06
NDUFS8	NADH dehydrogenase (ubiquinone) Fe-S protein 8	0.091	18.1	5.5	5.1	24.3	25.6	0.028	O00217	1	0.03
NDUFV1	NADH dehydrogenase (ubiquinone) flavoprotein 1	0.042	8.6	9.1	9.5	50.5	62.2	0.088	P49821	1	0.09
NDUFV2	NADH dehydrogenase (ubiquinone) flavoprotein 2	0.015	26.0	7.1	6.6	25.7	27.1	0.058	P19404	1	0.06
UQCRC1	ubiquinol-cytochrome c reductase core protein I	0.000	26.6	5.9	6.4	53.3	60.3	0.104	P31930	5	0.41
UQCRFS1	ubiquinol-cytochrome c reductase, Rieske iron-sulfur polypeptide 1	0.034	12.4	8.9	7.0	29.9	29.0	0.128	P47985	1	0.13
2.4. Energy Transduction											
CKM	creatine kinase, M chain	0.005	38.1	6.8	8.1	43.3	53.5	0.578	P06732	8	0.58
CKMT2	creatine kinase, sarcomeric mitochondrial	0.149	25.1	8.9	9.5	48.0	55.9	1.211	P17540	1	1.21
2.5. Lipid Metabolism/ß-Oxidation											
ALG1	ß-1,4 mannosyltransferase	0.129	14.7	5.6	4.7	26.5	35.2	0.023	Q9P2Y2	1	0.02
APOA1	apolipoprotein A-I	0.036	24.7	5.5	5.2	30.8	28.3	0.110	P02647	2	0.11
ECH1	enoyl co-enzyme A (CoA) hydratase 1, peroxisomal	0.006	16.2	8.7	7.8	36.1	36.9	0.021	Q13011	2	0.02
ECHS1	enoyl CoA hydratase 1, mitochondrial	0.020	21.0	8.9	6.9	31.8	31.3	0.020	P30084	1	0.02
FABP3	fatty acid-binding protein 3, muscle and heart	0.038	25.2	7.0	7.0	13.3	11.9	0.365	P05413	3	1.15
HMGCS1	hydroxymethylglutaryl-CoA synthase, cytoplasmic	0.160	11.9	5.8	7.3	56.0	83.2	0.031	Q01581	1	0.03
2.6. Nucleotide and Nucleic Acid Metabolism											
ADSS	adenylsuccinate synthase	0.043	8.0	8.8	6.0	50.2	52.7	0.034	P30520	1	0.03
AK1	adenylate kinase 1	0.084	23.0	7.8	9.5	21.9	25.5	0.121	P00568	1	0.12
DPYSL2	dihydropyrimidinase-like 2	0.085	12.4	6.0	7.3	62.7	74.3	0.038	Q16555	1	0.04
2.7. Other Metabolism Proteins											
ALDH2	aldehyde dehydrogenase, mitochondrial	0.010	0.2	6.6	6.2	56.3	65.8	0.070	P05091	1	0.07
GOLGA1	Golgi autoantigen (golgin 97)	0.019	12.0	5.2	5.7	88.3	88.4	0.042	Q92805	1	0.04
GOT1	aspartate aminotransferase 1	0.039	14.8	6.5	7.9	46.5	51.5	0.073	P17174	2	0.14
NSFL1C	p47 protein	0.082	17.3	5.1	5.9	41.1	66.5	0.037	Q9UNZ2	2	0.07
OXCT1	3-oxoacid CoA transferase 1 precursor	0.002	17.1	7.2	6.9	56.6	68.7	0.072	P55809	2	0.18
PSMD11	proteasome 26S non-ATPase subunit 11	0.087	17.3	5.5	7.5	43.2	74.3	0.019	O00231	1	0.02
PYGB	glycogen phosphorylase, brain form	0.001	15.3	6.5	7.5	99.5	86.8	0.017	P11216	1	0.02
TPI1	triosephosphate isomerase 1	0.054	22.2	6.5	8.1	26.8	28.7	0.018	P60174	2	0.04
3. Stress Response											
APTX	aprataxin	0.088	27.0	9.2	5.0	13.3	12.3	0.015	Q7Z2E3	1	0.02
CRYAB	crystallin, α B	0.010	44.0	6.8	7.6	20.1	22.6	1.865	P02511	5	1.86
CRYM	crystallin, mu	0.002	10.5	5.1	5.1	33.9	45.6	0.026	Q14894	3	0.03
DNAJC12	DnaJ (Hsp40) homolog, subfamily C, member 12	0.150	19.0	5.5	7.3	23.4	29.3	0.038	Q9UKB3	1	0.04
DNAJC13	DnaJ (Hsp40) homolog, subfamily C, member 13 (RME8)	0.022	18.5	8.4	7.0	50.6	61.3	0.020	O75165	1	0.02
GSTA1	glutathione S-transferase A1	0.073	31.1	5.4	6.2	23.3	26.9	0.030	P08263	1	0.03
HSPA5	heat shock 70-kDa protein 5	0.035	10.0	5.1	5.0	72.3	83.0	0.147	P11021	1	0.15
HSPA8	heat shock 70-kDa protein 8 isoform 2	0.000	35.6	5.6	5.8	53.6	77.7	0.234	P11142	5	0.87
HSPA9B	heat shock 70-kDa protein 9B precursor	0.002	30.2	6.0	5.7	74.1	79.4	0.194	P38646	6	0.70

Continued on next page

Table 1 continued.

Symbol	Description	Exp.[1]	Cov.[2] (%)	pI (T)	pI (E)	Mass (T)	Mass (E)	N. Vol.[3]	Accession number	No. Spots[4]	T. Vol.[5]
HSPB1	heat shock 27-kDa protein 1	0.074	36.6	8.1	5.7	22.4	30.4	0.219	P04792	8	0.64
HSPB6	heat shock protein, α-crystallin-related, B6	0.010	23.0	6.0	6.7	17.2	19.3	0.008	O14558	3	0.04
HSPB7	heat shock 27-kDa protein family, member 7 (cardiovascular)	0.007	32.1	5.4	5.2	15.5	12.2	0.011	Q9UBY9	1	0.01
HSPCA	heat shock 90-kDa protein 1, α	0.009	13.0	4.9	5.0	84.5	88.4	0.036	P07900	1	0.04
HSPD1	chaperonin (HSP60)	0.059	16.9	5.7	5.4	61.2	72.6	0.117	P10809	4	0.23
NOR1	oxidored-nitro domain-containing protein isoform 1	0.132	20.6	9.4	2.9	26.7	53.2	0.132	Q8N7G2	1	0.13
PDIA3	protein disulfide isomerase-associated 3	0.045	15.2	6.0	6.5	57.2	69.7	0.025	P30101	4	0.11
PRDX2	peroxiredoxin 2	0.002	28.0	5.2	5.4	18.5	24.4	0.125	P32119	3	0.23
PRDX6	peroxiredoxin 6	0.066	17.4	6.0	6.8	25.1	30.0	0.071	P30041	1	0.07
SERPINA1	α-1 antitrypsin	0.003	26.8	5.4	4.9	46.9	71.6	0.034	P01009	1	0.03
SOD1	superoxide dismutase 1, soluble	0.137	32.7	5.8	5.9	15.9	17.7	0.129	P00441	1	0.13
SOD2	superoxide dismutase 2, mitochondrial	0.000	32.3	6.9	7.7	23.7	23.7	0.148	P04179	3	0.23
TRA1	tumor rejection antigen (gp96) 1 (heat shock protein gp96)	0.008	9.1	4.7	4.7	90.4	95.0	0.043	P14625	1	0.04
4. Immune Response											
GZMA	granzyme A precursor	0.033	16.0	9.1	7.3	29.0	21.9	0.077	P12544	1	0.08
HLA-B	major histocompatibility complex, class I, B	0.130	12.0	6.1	7.8	40.5	31.2	0.040	P01889	1	0.04
HLA-G	major histocompatibility complex, class I, G	0.083	32.7	5.0	7.4	19.2	68.4	0.109	P17693	1	0.11
IGHG2	immunoglobulin heavy chain	0.028	31.7	5.2	6.8	35.9	43.3	0.026	P01859	2	0.16
TCRB	T cell receptor ß chain	0.002	32.7	6.5	9.5	19.9	26.9	0.081	P01850	2	0.10
5. Apoptosis											
CASP2	caspase-2 precursor	0.140	18.0	6.1	6.1	34.9	27.1	0.036	P42575	2	0.04
CASP8	caspase 8	0.100	12.0	5.7	6.4	30.7	26.7	0.061	Q14790	1	0.06
CTSD	cathepsin D (lysosomal aspartyl protease)	0.010	14.5	5.3	5.3	44.5	35.8	0.016	P07339	3	0.02
6. Cell Division and Proliferation											
FGFR3	fibroblast growth factor receptor 3	0.090	10.0	5.7	6.6	88.1	84.3	0.088	P22607	1	0.09
MLH1	DNA mismatch repair protein Mlh1	0.088	10.0	5.5	7.2	84.7	90.8	0.022	P40692	1	0.02
7. Cell Signaling and Control of Transcription and Translation											
FOXP4	forkhead box P4 isoform 1	0.086	24.8	4.5	7.8	16.2	80.8	0.014	Q8IVH2	1	0.01
GJE1	gap junction protein, epsilon 1, 29 kDa	0.031	17.0	9.4	6.7	31.3	60.8	0.065	Q8NFK1	2	0.08
PHB	prohibitin	0.002	37.5	5.6	5.9	29.9	34.3	0.042	P35232	2	0.06
TUFM	elongation factor Tu, mitochondrial precursor (EF-Tu) (P43)	0.020	19.0	7.9	7.3	49.9	56.8	0.052	P49411	3	0.15
8. Other Functions											
ALB	albumin precursor	0.057	17.3	5.6	6.2	68.4	76.0	6.653	P02768	5	6.65
ANXA5	annexin A5	0.090	16.6	4.9	4.9	35.8	41.0	0.024	P08758	1	0.02
ARFGAP1	ADP-ribosylation factor GTPase activating protein 1	0.032	27.8	4.4	5.6	44.7	46.1	0.019	Q8N6T3	1	0.02
C16orf49	chromosome 16 open reading frame 49 (unknown gene product)	0.020	25.2	5.6	4.9	35.7	43.8	0.026	O75208	3	0.03
CA1	carbonic anhydrase I	0.001	38.8	6.6	7.4	28.8	32.2	0.019	P00915	1	0.02
HBA1	hemoglobin, α1	0.026	14.1	9.1	9.4	15.0	11.2	0.274	P69905	2	0.29
HBB	hemoglobin, ß	0.002	40.6	6.8	7.8	15.0	11.5	0.101	P68871	2	0.20
IMMT	inner membrane protein, mitochondrial	0.000	9.0	6.1	6.5	83.6	84.2	0.112	Q16891	4	0.26
MB	myoglobin	0.018	44.2	7.9	3.1	17.2	15.5	1.120	P02144	7	3.79
MMP13	matrix metalloproteinase 13 (collagenase 3)	0.130	25.0	5.3	8.4	53.8	55.6	0.067	P45452	3	0.13
NUP153	nucleoporin 153 kDa	0.087	4.0	8.9	6.6	153.8	69.9	0.018	P49790	1	0.02
RTN1	reticulon 1	0.080	7.1	4.6	6.7	83.9	68.9	0.036	Q16799	1	0.04
TF	transferrin	0.040	7.9	7.1	7.0	79.3	82.4	0.336	P02787	3	0.50

[1]Expectation; [2]coverage; [3]normalized volume; [4]number of spots identified as the same protein; [5]total volume (total volume of all spots identified as the named protein). (E) = experimental; (T) = theoretical.

belonged to a metabolic pathway. Most of the proteins identified in this group were enzymes or enzyme subunits related to energy metabolism, belonging to the glycolysis (5 proteins), β-oxidation (2 proteins), tricarboxylic acid cycle (7 proteins) and electron transport and oxidative phosphorylation (11 proteins) pathways. As examples, aconitase, fumarate hydratase, pyruvate dehydrogenase, and enolase play important roles in the tricarboxylic acid cycle and NADH dehydrogenase isoforms and cytochrome c reductase are subunits of the complexes from the respiratory chain. We also identified members of the energy transduction (creatine kinase) pathway; significantly, a high number of spots were identified as creatine kinase M isoforms (Table 1, Figure 1), which catalyzes the transphosphorylation reaction of mitochondrial ATP to phosphocreatine and ADP for cytoplasmic ATP synthesis (18). The creatine kinase pathway is an important complementary pathway under conditions of high ATP demand (19). We also identified other members of the lipid metabolism pathway, as well as three proteins involved in nucleotide/nucleic acid metabolism.

The identification of a significant number of proteins involved in stress (19%), in the immune response (4%) and in apoptotic (3%) processes reinforces their importance in the pathogenesis of CCC. Among the stress proteins, the most frequently identified were heat shock proteins (HSP) and cognates. In the present study, 10 HSP were identified (isoforms of HSP27, HSP40, HSP60, HSP70, and HSP90). Crystallin is also a member of this protein superfamily (20). Oxidative stress-related proteins such as peroxiredoxin and both Cu/Zn and Mn superoxide dismutases were also frequently identified; these proteins are antioxidants and protect the cell against free radicals, especially reactive oxygen intermediates (21).

Analysis of the proteomic profile of the CCC myocardium also identified proteins

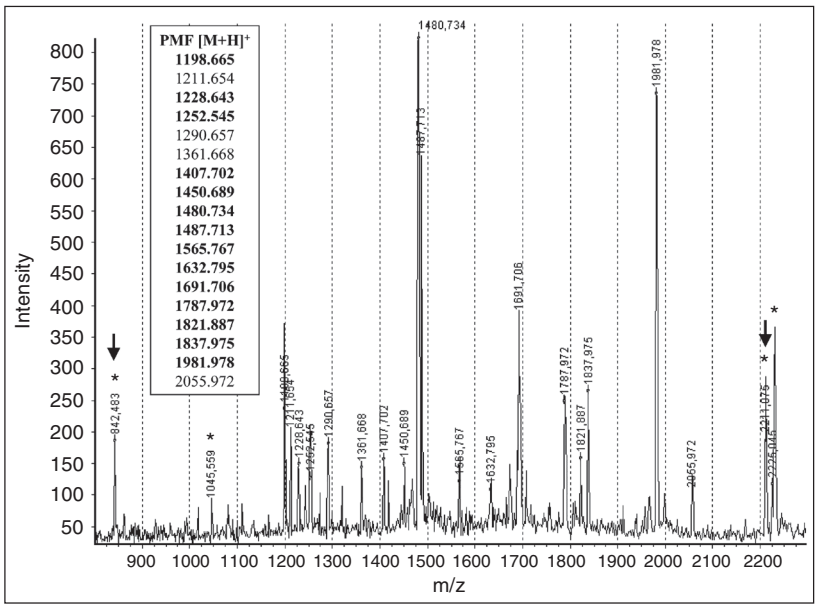

Figure 2. MALDI-ToF mass spectrum of the tryptic products from a spot. The peptide mass fingerprinting (PMF) list used for protein identification in the databanks is shown. *Trypsin autolysis peptides used for internal calibration. Peaks that appeared in all spectra were not included in the PMF list. In bold, the m/z values from the PMF list that were matched with the identified protein from the database. This spectrum was identified as a heat shock 70-kDa protein 8 isoform 2 (expectation: 0.003, coverage: 37.1%) using the non-redundant NCBI databank (*Homo sapiens*).

Table 2. Functional classification of the proteins identified in the myocardium from patients with chronic Chagas' disease cardiopathy.

Functional classification	%
1. Structural and contractile proteins	19
2. Metabolism	38
2.1. Glycolysis	12
2.2. Tricarboxylic acid cycle	17
2.3. Oxidative phosphorylation and electron transport	26
2.4. Energy transduction	5
2.5. Lipid metabolism/ß oxidation	14
2.6. Nucleotide and nucleic acid metabolism	7
2.7. Other metabolism proteins	19
3. Stress response	20
4. Immune response	4
5. Apoptosis	3
6. Cell division and proliferation	2
7. Cell signaling and control of transcription and translation	4
8. Other functions	12

The functional classification of the identified proteins was adapted from the Gene Ontology classification using the FatiGO tool (http://fatigo.bioinfo.cipf.es).

related to the immune system, such as immunoglobulins, T cell receptor ß chain, HLA class I molecule, and granzyme A. The expression of HLA class I and granzyme A is increased expression in the myocardium from CCC patients (7,8). Granzyme A, a protein known to be produced by CD8+ cytotoxic T cells - which are highly abundant in CCC myocardium (22) - triggers apoptosis of target cells in the presence of CD8+ T cell cytotoxicity (23). Regarding proteins related to the apoptotic process, we found caspases 2 and 8 in CCC heart whose sequential activation plays a central role in cell apoptosis (24).

Proteins related to cell division and proliferation and related to cell signaling and to the control of transcription and translation were 2 and 4% of the identified proteins, respectively. Some of these proteins were: prohibitin, which plays a role in regulating proliferation and inhibits DNA synthesis (25), Forkhead box P4 isoform 1, which is a transcriptional repressor that has been involved in cardiac morphogenesis (26), and protein disulfide isomerase-associated 3, which is classified as a signal transduction protein, but which could also be classified as an electron transport protein and plays a role in the oxidative process (27).

Several spots from the CCC gels, with different pI and mass, were identified by PMF as the same protein, such as aconitase, creatine kinase M chain, and heat shock 70-kDa protein, which were identified in 7, 8, and 6 spots, respectively. Structural and contractile proteins, such as several forms of actin (ACTA1, ACTA2, ACTC, ACTG2, ACTN2), desmin, myosin (MYL3 and MYL7), and vimentin were also identified with different pI values. These could be a result of post-translational modifications such as oxidation, phosphorylation, acetylation, or other processes. Some proteins presented differences in both mass and pI compared to the Swiss-Prot database, such as class I major histocompatibility complex G (HLA-G), which shows a difference between the experimental and theoretical value of 2.4 pI units, while the theoretical mass was 49 kDa less than the experimental mass. The same occurred with immunoglobulin heavy chain (IGHG2) which showed a difference between the experimental and theoretical value of 1.6 pI units, and the theoretical mass was 7.4 kDa less than the experimental mass.

In order to validate the mass spectrometric identification of proteins, we selected 5 representative identified proteins (caspase 8, caspase 2, hsp60, Cu/Zn superoxide dismutase, and protein disulfide isomerase 3) for further analysis by immunoblot with the aid of specific monoclonal antibodies, in tissue samples from 6 CCC patients (Figure 3). We identified protein bands of the expected molecular weights reacting with the 5 specific antibodies in all samples tested, con-

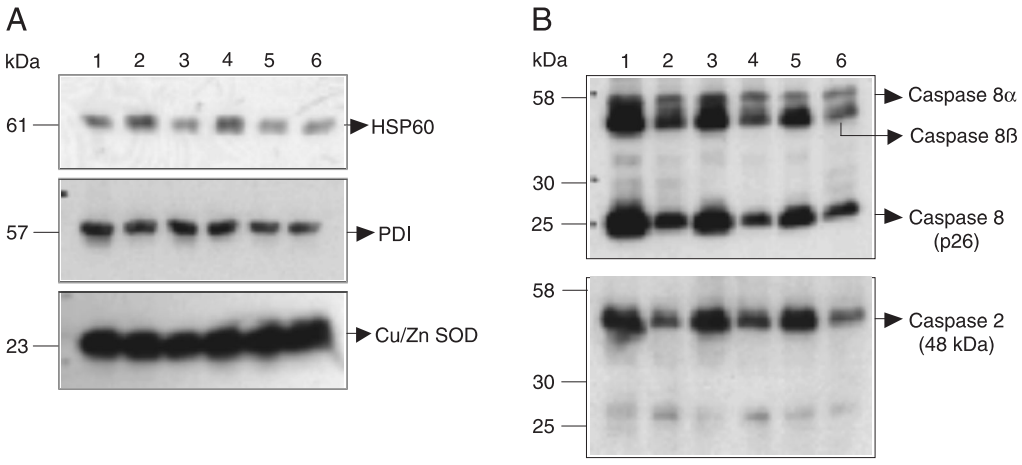

Figure 3. Validation of selected proteins by Western blot analysis of 6 myocardium samples from patients with chronic Chagas' disease cardiopathy. *A*, Identification of HSP60 (61 kDa), PDI (~55 kDa) and CuZn SOD (~23 kDa), which are involved in the oxidative stress process. *B*, Identification of apoptotic proteins, α and ß caspase 8 (~58 kDa) and caspase 2 (48 kDa). The processed form of caspase 8 (~26 kDa) was also identified. HSP = heat shock protein; PDI = protein disulfide isomerase; SOD = superoxide dismutase.

firming the existence of proteins identified by PMF. Furthermore, we observed the processed forms of caspase 8, indicating its possible activation.

Discussion

We describe the protein profile of the myocardium from patients with chronic Chagas' disease cardiomyopathy. To our knowledge, although data from several differential proteome analyses in myocardial samples are available in the literature, the present study is the first report on the myocardial protein profile of CCC patients. Besides identifying the abundant structural and contractile myocardial proteins, this approach allowed us to identify proteins not expected to be found in normal myocardium, such as stress and oxidative stress proteins, apoptosis effector molecules and proteins involved in the immune response.

Structural proteins such as sarcomeric actomyosin complex constituents, as well as cytoskeletal proteins, were frequently identified, as expected, since sarcomeric contractile proteins are the most abundant proteins in the myocardium. Among the structural proteins, the atrial isoform of MYL4 was identified in the CCC ventricle samples. Ventricular expression of atrial proteins has been observed in cardiac hypertrophy and has been ascribed to reversal of myocytes to an embryonic program of gene transcription (16). Vimentin, highly expressed in fibroblasts, was also identified, in agreement with the intense fibrotic process known to occur in CCC heart tissue (17). We could also identify matrix metalloproteinase 13 (MMP13), also called collagenase-3, which is expressed by different cell types including stromal fibroblasts. MMP13 degrades collagens I, II, III, gelatin, fibronectin, laminin, and tenascin (28). Other MMP such as MMP9 (29) has been reported to play a role in cardiac remodeling. Thus, we may suggest that MMP13 could also be involved in the intense remodeling that occurs in the CCC myocardium.

The finding that 27% of the identified proteins belong to the different pathways of energy metabolism that directly participate in the generation of ATP (glycolysis, ß-oxidation, tricarboxylic acid cycle, oxidative phosphorylation, and creatine kinase system) (Table 1) is consistent with the fact that the heart requires significant energy for normal cardiac function (19,30). Moreover, most of the cardiac diseases in which mechanical dysfunction development occurs are associated with a deficit in energy production, often generated by disturbances in one or more metabolic steps of the ATP production pathways (19).

A significant number of HSP and cognates (40 spots, 13 distinct HSP) were identified in CCC myocardium. Transient HSP synthesis protects cellular homeostasis after exposure to heat and to a wide spectrum of stressful and potentially deleterious stimuli (31,32). Accumulating evidence has implicated HSPs as mediators of myocardial protection, particularly in experimental models of ischemia and reperfusion injury (31). Different protective functions have been attributed to HSPs, including repairing ion channels, restoring redox balance, interacting with nitric oxide-induced protection, inhibiting proinflammatory cytokines, and preventing activation of the apoptosis pathway (31). The significant number of spots identified as HSPs in the CCC samples supports their role in myocardial protection. We could identify 12 spots as isoforms of HSP70, which is expressed at low levels in normal tissue and is rapidly induced in response to ischemic stress (33). The increase in myocardial HSP60 production has also been associated with the development of chronic heart failure (32).

Multiple spots were identified as oxidative stress-related proteins, such as peroxiredoxin and both Cu/Zn and Mn superoxide dismutase. Studies on animal models have

suggested that a chronic increase in oxidative stress in the myocardium, possibly due to impairment of superoxide dismutase and other antioxidant pathways, could contribute to myocardial remodeling and failure (34). A murine model of *T. cruzi* infection showed that the progressive severity of disease of infected mice is associated with increased oxidative damage in the myocardium, which seems to result from enhanced oxidant production coupled with diminishing antioxidant defense (35).

Proteins that play a role in immune processes were also detected in CCC myocardium. T cell receptor and immunoglobulin are consistent with the mononuclear infiltrate that is a hallmark of CCC. Moreover, these findings are technically interesting, since 2-D gel electrophoresis/PMF proteomic analysis is expected to identify only the most abundantly expressed proteins from the cardiac cells, rather than proteins from a comparatively small infiltrating inflammatory cell population observed in CCC myocardium. We also identified granzyme A, that initiates an alternative pathway for granule-mediated apoptosis (36) and is one of the three key components of the lytic granules of CD8+ T cells, which constitute the majority of the mononuclear infiltrate (22). However, one cannot rule out the possibility that these findings are due to blood contamination.

In our profile experiment we found caspases 2 and 8. Caspase 8 plays a role in CD95- and tumor necrosis factor-induced cell death (24). Apoptosis has been associated with heart damage in numerous diseases, such as viral infection, myocardial infarction, diabetes, and regression of hypertrophy (37,38). Apoptosis assessed by the TUNEL method has been shown in CCC, and myocardial cell loss by apoptosis may contribute to heart failure (39). This is reinforced by the identification of activated caspase 8 forms in all 6 CCC myocardium samples (Figure 3).

The observation of several spots identified by PMF as the same protein, but showing distinct pI's may represent different isoforms of the protein, post-translational modifications or technical artifacts of the 2-D methodology. Post-translational modifications such as phosphorylation or acetylation may be visualized on 2-D electrophoresis gels as a "train of spots" differing only by their pI, and have been observed previously by other investigators. These protein modifications were not characterized in the present study, but such trains of spots were observed in some structural and contractile proteins such as several forms of actin (ACTA1, ACTA2, ACTC, ACTG2, ACTN2), desmin, MYL3 and MYL7, and vimentin, that were identified with different pI values. Other spots from the CCC gels, with different pI and mass, were also identified as the same protein, such as aconitase, creatine kinase M chain, and heat shock 70-kDa protein that were identified in 7, 8, and 6 spots, respectively. The reason for this large number of isoforms shown by some proteins is not known. Literature data suggest that a subset of proteins from cardiac mitochondria appear to be susceptible to double oxidation of their tryptophan residues (40). The fact that some proteins presented differences between experimental and theoretical mass and pI (e.g., HLA-G and IGHG2) could be due to the matching with sequence fragments in the databanks, rather than complete protein sequences.

Several isoforms of the same protein showing distinct experimental mass and pI may also represent hydrolytic fragments formed during breakdown of the parent molecules *in vivo* or *in vitro*, with oxidation forms resulting from the 2-D gel processing and precursors arising during protein assembly. Another limitation of the present study was that the proteins identified here may not originate from the cardiac tissue itself. As in most mammalian organs, the involvement of vascular tissue needs to be considered, and this may explain the identification of

smooth muscle forms of actin. Blood-derived proteins were also found, including albumin, hemoglobin and transferrin.

Proteomic analysis including 2-D gel electrophoresis and PMF has allowed us to identify 246 matched protein spots, representative of 112 distinct proteins, in myocardial tissue from end-stage CCC patients. This paper has described for the first time a significant expression of oxidative stress and apoptosis-related proteins in CCC heart tissue, suggesting the possible participation of such processes in CCC pathogenesis, a subject that is currently under investigation.

Acknowledgments

The authors thank Dr. Mario Palma (Universidade Estadual de São Paulo, Rio Claro, SP, Brazil) and Drs. Simone Fonseca, Angelina Bilate and Kellen Fae (Universidade de São Paulo, São Paulo, SP, Brazil) for critical readings and discussion.

References

1. Morel CM, Lazdins J. Chagas disease. *Nat Rev Microbiol* 2003; 1: 14-15.
2. Bestetti RB, Muccillo G. Clinical course of Chagas' heart disease: a comparison with dilated cardiomyopathy. *Int J Cardiol* 1997; 60: 187-193.
3. Freitas HF, Chizzola PR, Paes AT, Lima AC, Mansur AJ. Risk stratification in a Brazilian hospital-based cohort of 1220 outpatients with heart failure: role of Chagas' heart disease. *Int J Cardiol* 2005; 102: 239-247.
4. Higuchi ML, De Morais CF, Pereira Barreto AC, Lopes EA, Stolf N, Bellotti G, et al. The role of active myocarditis in the development of heart failure in chronic Chagas' disease: a study based on endomyocardial biopsies. *Clin Cardiol* 1987; 10: 665-670.
5. Reis MM, Higuchi ML, Benvenuti LA, Aiello VD, Gutierrez PS, Bellotti G, et al. An *in situ* quantitative immunohistochemical study of cytokines and IL-2R in chronic human chagasic myocarditis: correlation with the presence of myocardial *Trypanosoma cruzi* antigens. *Clin Immunol Immunopathol* 1997; 83: 165-172.
6. Abel LC, Rizzo LV, Ianni B, Albuquerque F, Bacal F, Carrara D, et al. Chronic Chagas' disease cardiomyopathy patients display an increased IFN-gamma response to *Trypanosoma cruzi* infection. *J Autoimmun* 2001; 17: 99-107.
7. Reis DD, Jones EM, Tostes S Jr, Lopes ER, Gazzinelli G, Colley DG, et al. Characterization of inflammatory infiltrates in chronic chagasic myocardial lesions: presence of tumor necrosis factor-alpha+ cells and dominance of granzyme A+, CD8+ lymphocytes. *Am J Trop Med Hyg* 1993; 48: 637-644.
8. Reis DD, Jones EM, Tostes S, Lopes ER, Chapadeiro E, Gazzinelli G, et al. Expression of major histocompatibility complex antigens and adhesion molecules in hearts of patients with chronic Chagas' disease. *Am J Trop Med Hyg* 1993; 49: 192-200.
9. Cunha-Neto E, Kalil J. Heart-infiltrating and peripheral T cells in the pathogenesis of human Chagas' disease cardiomyopathy. *Autoimmunity* 2001; 34: 187-192.
10. Teixeira MM, Gazzinelli RT, Silva JS. Chemokines, inflammation and *Trypanosoma cruzi* infection. *Trends Parasitol* 2002; 18: 262-265.
11. Gomes JA, Bahia-Oliveira LM, Rocha MO, Martins-Filho OA, Gazzinelli G, Correa-Oliveira R. Evidence that development of severe cardiomyopathy in human Chagas' disease is due to a Th1-specific immune response. *Infect Immun* 2003; 71: 1185-1193.
12. Cunha-Neto E, Dzau VJ, Allen PD, Stamatiou D, Benvenutti L, Higuchi ML, et al. Cardiac gene expression profiling provides evidence for cytokinopathy as a molecular mechanism in Chagas' disease cardiomyopathy. *Am J Pathol* 2005; 167: 305-313.
13. Arrell DK, Neverova I, Van Eyk JE. Cardiovascular proteomics: evolution and potential. *Circ Res* 2001; 88: 763-773.
14. Sutton CW, Pemberton KS, Cottrell JS, Corbett JM, Wheeler CH, Dunn MJ, et al. Identification of myocardial proteins from two-dimensional gels by peptide mass fingerprinting. *Electrophoresis* 1995; 16: 308-316.
15. Smith PK, Krohn RI, Hermanson GT, Mallia AK, Gartner FH, Provenzano MD, et al. Measurement of protein using bicinchoninic acid. *Anal Biochem* 1985; 150: 76-85.
16. Schwartz K, Boheler KR, de la Bastie D, Lompre AM, Mercadier JJ. Switches in cardiac muscle gene expression as a result of pressure and volume overload. *Am J Physiol* 1992; 262: R364-R369.
17. Rossi MA. The pattern of myocardial fibrosis in chronic Chagas' heart disease. *Int J Cardiol* 1991; 30: 335-340.
18. Wallimann T. Dissecting the role of creatine kinase. *Curr Biol* 1994; 4: 42-46.
19. Carvajal K, Moreno-Sanchez R. Heart metabolic disturbances in cardiovascular diseases. *Arch Med Res* 2003; 34: 89-99.
20. Ingolia TD, Craig EA. Four small *Drosophila* heat shock proteins are related to each other and to mammalian alpha-crystallin. *Proc Natl Acad Sci U S A* 1982; 79: 2360-2364.
21. Nordberg J, Arner ES. Reactive oxygen species, antioxidants, and the mammalian thioredoxin system. *Free Radic Biol Med* 2001; 31: 1287-1312.
22. Higuchi MD, De Brito T, Reis MM, Bellotti G, Pereira-Barretto AC, Pileggi F. Correlation between *T. cruzi* parasitism and myocardial inflammatory infiltrate in human chronic chagasic myocarditis: light microscopy and immunohistochemical findings. *Cardiovasc Pathol* 1993; 2: 101-105.
23. Pardo J, Bosque A, Brehm R, Wallich R, Naval J, Mullbacher A, et al. Apoptotic pathways are selectively activated by granzyme A and/or granzyme B in CTL-mediated target cell lysis. *J Cell Biol* 2004; 167: 457-468.
24. Cohen GM. Caspases: the executioners of apoptosis. *Biochem J* 1997; 326 (Pt 1): 1-16.

25. Mishra S, Murphy LC, Nyomba BL, Murphy LJ. Prohibitin: a potential target for new therapeutics. *Trends Mol Med* 2005; 11: 192-197.
26. Li S, Zhou D, Lu MM, Morrisey EE. Advanced cardiac morphogenesis does not require heart tube fusion. *Science* 2004; 305: 1619-1622.
27. Janiszewski M, Lopes LR, Carmo AO, Pedro MA, Brandes RP, Santos CX, et al. Regulation of NAD(P)H oxidase by associated protein disulfide isomerase in vascular smooth muscle cells. *J Biol Chem* 2005; 280: 40813-40819.
28. Creemers EE, Cleutjens JP, Smits JF, Daemen MJ. Matrix metalloproteinase inhibition after myocardial infarction: a new approach to prevent heart failure? *Circ Res* 2001; 89: 201-210.
29. Ducharme A, Frantz S, Aikawa M, Rabkin E, Lindsey M, Rohde LE, et al. Targeted deletion of matrix metalloproteinase-9 attenuates left ventricular enlargement and collagen accumulation after experimental myocardial infarction. *J Clin Invest* 2000; 106: 55-62.
30. Corbett JM, Why HJ, Wheeler CH, Richardson PJ, Archard LC, Yacoub MH, et al. Cardiac protein abnormalities in dilated cardiomyopathy detected by two-dimensional polyacrylamide gel electrophoresis. *Electrophoresis* 1998; 19: 2031-2042.
31. Delogu G, Signore M, Mechelli A, Famularo G. Heat shock proteins and their role in heart injury. *Curr Opin Crit Care* 2002; 8: 411-416.
32. Tanonaka K, Yoshida H, Toga W, Furuhama K, Takeo S. Myocardial heat shock proteins during the development of heart failure. *Biochem Biophys Res Commun* 2001; 283: 520-525.
33. Marber MS, Mestril R, Chi SH, Sayen MR, Yellon DM, Dillmann WH. Overexpression of the rat inducible 70-kD heat stress protein in a transgenic mouse increases the resistance of the heart to ischemic injury. *J Clin Invest* 1995; 95: 1446-1456.
34. Dhalla AK, Hill MF, Singal PK. Role of oxidative stress in transition of hypertrophy to heart failure. *J Am Coll Cardiol* 1996; 28: 506-514.
35. Wen JJ, Vyatkina G, Garg N. Oxidative damage during chagasic cardiomyopathy development: role of mitochondrial oxidant release and inefficient antioxidant defense. *Free Radic Biol Med* 2004; 37: 1821-1833.
36. Shresta S, Graubert TA, Thomas DA, Raptis SZ, Ley TJ. Granzyme A initiates an alternative pathway for granule-mediated apoptosis. *Immunity* 1999; 10: 595-605.
37. Frustaci A, Kajstura J, Chimenti C, Jakoniuk I, Leri A, Maseri A, et al. Myocardial cell death in human diabetes. *Circ Res* 2000; 87: 1123-1132.
38. Freude B, Masters TN, Kostin S, Robicsek F, Schaper J. Cardiomyocyte apoptosis in acute and chronic conditions. *Basic Res Cardiol* 1998; 93: 85-89.
39. Tostes S Jr, Bertulucci Rocha-Rodrigues D, de Araujo Pereira G, Rodrigues V Jr. Myocardiocyte apoptosis in heart failure in chronic Chagas' disease. *Int J Cardiol* 2005; 99: 233-237.
40. Taylor SW, Fahy E, Murray J, Capaldi RA, Ghosh SS. Oxidative post-translational modification of tryptophan residues in cardiac mitochondrial proteins. *J Biol Chem* 2003; 278: 19587-19590.